

Aerodynamics for Optimal Engine-Integrated Airbreathing Launcher Configurations

Mark J. Lewis¹

University of Maryland, College Park MD 20742-3015

Iain D. Boyd²

University of Michigan, Ann Arbor, MI 48109-2140

Charles E. Cockrell, Jr.³

NASA Langley Research Center, Hampton VA 23661-2101

An overview of some of the activities in hypersonic airbreathing aerodynamics and propulsion airframe integration is presented for the Space Vehicle Technology Institute. The Institute is a multi-university joint NASA-DoD program that was created as a center for research and education in future launch vehicle technologies. Perhaps more than any other type of flight vehicle, next generation space launchers will have to be analyzed as completely integrated aerodynamic-propulsion systems. Optimal aerodynamics will be vital to the development of efficient, engine-integrated launch vehicle forms, especially using airbreathing propulsion. To this end, inverse design approaches, design tradeoffs, and an understanding of relevant basic flow physics are all part of the Space Vehicle Technology Institute program. The relevance of these efforts to NASA activities is also described.

I. Introduction

AMONG the challenges in launch vehicle design is balancing the integrated requirements for practical propulsion with good volumetrics, structural efficiency, controllability, and heating survivability. For airbreathing vehicles, or those with extended reentry footprints, coupled aerodynamic performance is also vital. The degree of coupling and close integration raises many questions about practical aerodynamic designs for hypersonic flight.

Of all future launch concepts, hypersonic airbreathers will have their own special propulsion-airframe integration challenges. For cruisers, it is well-known that the optimal propulsion system is one that maximizes the range by providing the highest product of specific impulse and lift-over-drag, L/D for a given fuel weight fraction. Airbreathers that consume large fractions of their weight are not strictly governed by the Breguet range equation, but the general trends of that simple formulation are still valid.¹ This will generally favor designs in which the engine contributes to lift, and where inlet efficiency is absolutely critical.² Lift-over-drag is as important as specific impulse for the performance of such vehicles.³ Though accelerators are different than atmospheric cruisers, there are some analogies to be drawn.

Accelerators, including airbreathing access-to-space vehicles, achieve maximum overall performance with greatest *effective* specific impulse, realized with the maximum difference between thrust and drag. This translates into the need to design efficient engine systems on low-drag airframes. Note that horizontal launchers, including airbreathing accelerators, will match lift to weight, and so must also have high L/D in horizontal flight.

This need for high lift on horizontal vehicles stands in stark contrast to the requirements for vertical launch, especially with traditional rockets. In that case, drag represents a very small fraction of overall energy loss in flight to orbital speed, 7790 m/sec; the space shuttle velocity loss to gravity (1220 m/s) is over ten times greater than losses due to drag (118 m/s). In contrast, a horizontal launcher would have negligible gravity losses and drag losses will dominate.

Reentry vehicles may derive significant benefit from higher L/D for extended landing footprint and maneuvering. A wide range of space missions may be enabled with high lift, low drag aerodynamic shapes. These

¹ Professor, Department of Aerospace Engineering, Fellow AIAA

² Professor, Department of Aerospace Engineering, Associate Fellow AIAA

³ Aerosciences Technology Manager, Mail Stop 173, Senior Member AIAA

include aerodynamic plane change, aerodynamic gravity assist for planetary trajectories, and maneuverable reentry with extended, lower-peak heating rates.

All of these issues are driving factors in the research program of the Space Vehicles Technology Institute.

A. NASA and DoD Launcher Aerodynamic Interests

The research activities of the SVT Institute are formulated to be supportive and complementary to those of NASA and the DoD sponsors. NASA in particular has been pursuing research and technology for airframe-integrated launch vehicle applications, specifically concepts utilizing hypersonic airbreathing propulsion.

A NASA team has completed an assessment of technologies required to support future hypersonics system development in a re-focused program. The re-formulated plans are intended to continue development of hypersonics technology in support of future airbreathing launch vehicle applications. The initial reference system focus is based on a two-stage-to-orbit (TSTO) launch vehicle system that utilizes high-speed turbomachinery and ramjet or dual-mode scramjet propulsion. A spiral development approach has been proposed to systematically increase the staging Mach number and, eventually, to develop technologies applicable to single-stage-to-orbit (SSTO) vehicles. Similar concepts are under study in the SVTI.

Many of the technology challenges identified by NASA in the area of aerodynamics, aerothermodynamics and propulsion-airframe integration are well-supported by activities in the SVTI. Others represent long-term goals of SVTI activities. High-priority technical challenges include:

- Continued development of high-fidelity design tools capable of modeling flow physics of powered hypersonic configuration in the transonic speed regime. An objective is to mature these validated tools for inclusion in early conceptual design cycles.
- Validation of tools and test techniques for proximity aerodynamic assessments during stage separation of TSTO hypersonic configurations.
- Demonstration of inlet and engine mode transition between propulsion system operating modes and assessment of dynamic effects on aerodynamic forces and moments.
- Assessments of vehicle stability and control due to engine dynamics, failures or aero-propulsion modeling uncertainties.
- Development of advanced computational tools for tip-to-tail flowpath analysis, vehicle performance and aeroheating analyses. This includes physics-based modeling for boundary-layer transition, localized heating effects due to shock-boundary layer interaction and shock impingement, and other flow phenomena.
- Continued development of hypersonic flow control mechanisms. Examples may include the use of mass injection for boundary layer control to improve control surface effectiveness and the use of passive porosity for hypersonic laminar flow control.
- Continued maturation of powered simulation test techniques at hypersonic speeds. A significant gap in this area is the ability measure aerodynamic forces and moments on powered vehicle configurations in pulse facilities used for hypervelocity ground testing.

B. Flight Test Experience

NASA has already gained hypersonic flight experience with the X-43A, which successfully demonstrated an airframe-integrated, scramjet-powered vehicle at Mach 7 flight conditions in March 2004.⁴ This program has generated substantial analysis, ground test data and flight test data regarding aero-propulsive performance, aerothermodynamics, and propulsion-airframe integration characteristics of hypersonic airbreathing configurations. Computational predictions, wind tunnel testing, and full-flowpath propulsion ground tests were obtained to develop an aerodynamics database for the X-43A vehicle along the nominal mission profile. Boundary-layer transition phenomena were also studied in pre-flight predictions and wind tunnel testing, as was the effectiveness of forced transition mechanisms.

The University Institute program of which the Space Vehicles Technology Institute is a part was actually developed under the Next Generation Launch Technology (NGLT) program. The NGLT program was aimed at developing technologies for reusable launch vehicles (RLV), including hypersonic airbreathing concepts.⁵ A

description of research and technology in the areas of aerodynamics, aerothermodynamics, aero-propulsion integration and flight mechanics is described in reference 5. Ground and flight technology demonstrations were also part of the program, such as the X-43C hypersonic flight demonstrator program, which was to be conducted as a joint program with the U.S. Air Force to demonstrate ramjet-to-scramjet transition in an airframe-integrated hypersonic configuration.⁶ The NGLT program was cancelled to re-focus resources and technology development within NASA towards the Vision for Space Exploration. However, during the conduct of this program, accomplishments in several research areas were achieved. Several future reusable combined-cycle flight demonstrator concepts were studied to demonstrate combined turbomachinery and dual-mode scramjet propulsion in an integrated vehicle system. Work also proceeded on issues related to transonic drag, as hypersonic airbreathers can have particular difficulties accelerating through Mach 1⁷.

The NGLT program also saw significant advancements in the development of computational tools to simulate moving-body aerodynamic separation problems. This is especially applicable to TSTO concepts, such as the reference rocket-based TSTO configuration, referred to as the Langley Glideback Booster (LGBB) that was used for NASA studies.⁸ Investigation into boundary layer transition phenomena and advancements in physics-based transition modeling were accomplished. The ability of airbreathing systems to achieve positive net thrust is dependent on a small difference between large thrust and drag components at high Mach numbers. Therefore, large uncertainties in transition location could result in increased drag and decreased performance margin.⁹ Efforts to improve transition prediction models include the application of linear stability theory to hypersonic transition and examination of data from the Pegasus flight experiment.^{10,11} As a follow-on to the development and characterization of passive forced transition mechanisms for the X-43A flight experiment, alternative mechanisms that can provide “transition on demand” were investigated. The approach of using mass injection to force boundary layer transition was demonstrated experimentally at Mach 6 and Mach 10 conditions.¹²

There is an interest in three-dimensional flowpath concepts for enhanced performance of hypersonic airbreathing systems, especially in the Mach 3-8 speed regime. Interest in these configurations is driven by perceived advantages relative to forebody-inlet integration, reduced drag and heat load for elliptic combustors and elimination of corner flows in isolators and combustors, thereby providing potential improvements in installed performance. Smart previously demonstrated inlet performance at Mach 4 and 6 test points in a rectangular-to-elliptic-shape transition (REST) design.¹³ This shape is designed for integration in traditional two-dimensional and lifting-body vehicle designs, while providing the benefits of elliptic combustors. Full flowpath performance of a reference design will be demonstrated in combustion testing. Sabean and Lewis investigated a similar 2-D to -3-D flowpath using computational optimization.¹⁴

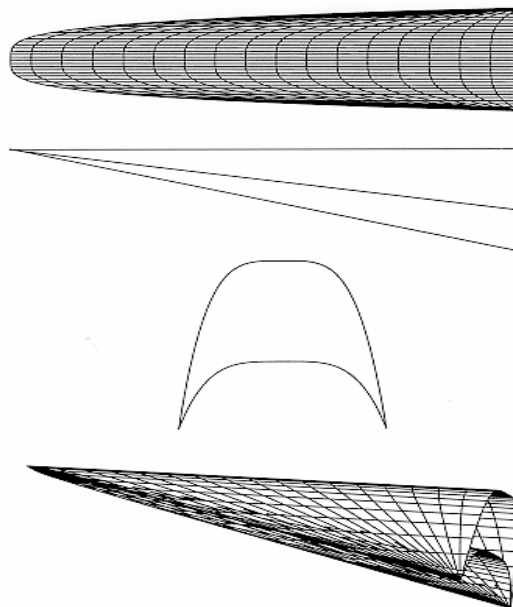


Figure 1. Typical waverider shape derived for on-design shock attachment, high volume, and maximum L/D . Ref. 16.

II. Applied Aerodynamics

Work in the SVTI has sought to complement interests and key challenges in NASA and DoD activities. Among these areas is applied aerodynamics.

A. Inverse Aerodynamic Design

The basic nature of hypersonic flows can be used to advantage in taking an “inverse” approach to integrated vehicle design, in which a desired flowfield is first selected, and then an associated airframe/engine combination is defined. One class of inverse solutions is derived through the use of the so-called “waverider” geometries. The Space Vehicle Technology Institute is currently exploring several research avenues that exploit such an approach, as well as examining the basic physics of low-drag aerodynamic forms.

Waveriders are supersonic shapes in which the bow shockwave is directly attached to the leading edge. This means that all of the flow that passes through the shockwave on the lower lifting part of the waverider is contained below the waverider. This has the benefit of producing a generally high value of available L/D with high lift, and

reducing cross flow and non-uniformities on the compression surface. It also provides for efficient capture into an inlet. Waveriders were first defined by Nonweiler.¹⁵ They can be designed directly¹⁶ such as the shape in Fig. 1, or generated by starting with a known flow with a given shockwave; a stream surface parallel to the direction of flow under the wedge is selected to represent the lower surface of the waverider. The intersection of that lower surface and the original shockwave defines the leading edge with an attached shockwave. This process works because the flowfield is mathematically hyperbolic, so that the carved-out section, which forms the waverider surface, representing perhaps a small portion of the original flowfield, still retains the properties of that flowfield even though the generating body has been ignored once the waverider is defined.

Nonweiler's original work used simple wedge flows to form the shockwave because of their ease of calculation. Other generating bodies can also be used as the starting point of the waverider flowfield design process. Conically-derived waveriders have been used extensively because they tend towards higher volumetric efficiency than the wedge-derived forms. Combinations of cones and wedges have also been explored for creating the generating flowfield.¹⁷ For a given flight Mach number, both the wedge and cone-shaped forms have only one degree of freedom: the oblique surface angle. In fact, nearly any shape that has associated with it a shockwave and supersonic downstream flow can be used as the initial generating body for a waverider. In turn, each flowfield contains an infinite number of stream surfaces from which to form the final waverider.

There is no known directed methodology for selecting the best initial generating form for a given application, since the optimal waverider is derived with only a portion of the generating flowfield – e.g. a minimum drag generating body may not yield a low-drag waverider, as the waverider may be optimized in a portion of the flowfield far removed from the original surface. Current work has concentrated on modifying and validating a technique that eliminates the need to choose a generating body and permits direct specification of the desired shock wave instead. This is the so-called osculating (Latin for "kissing") cones waverider method developed originally by Sobieczky and explored by Takashima and Lewis.¹⁸

In the method of osculating cones, the generating flow is defined by a design Mach number, a bow shock angle, and a shock wave shape at the exit plane of the waverider. As a result, the method does not require a generating body to be defined. The flow field behind the non-axisymmetric shock is determined by assuming "locally conical" flow in the normal planes along the shock curve. The "locally conical" flow is defined by an osculating (Latin for "kissing") slice of flowfield. The vertex of the conical flowfield in each plane is determined by the local radius of curvature and the shock angle. The shock curve is chosen so that the change in the radius of curvature is continuous along the curve, and a series of planes is used along the shock curve in the exit plane to fully define the flow field behind the bow shock.

Since the flow field is assumed to be "locally axisymmetric," the osculating cones method can be inaccurate when large spanwise pressure gradients are present, such as the half waverider shown in Fig. 2. Current work has been examining ways to correct the transverse pressure gradients introduced into the osculating cone solutions as a result of varying shock curvature. The osculating cone solution builds a flowfield from axial slices of conical flow. The properties of the shocklayer in each slice are derived from the Taylor-Maccoll equations¹⁹:

$$\frac{d^2 \bar{V}_r}{d\theta^2} = \frac{\bar{V}_r \bar{V}_\theta^2 - \frac{\gamma-1}{2} (1 - \bar{V}_r^2 - \bar{V}_\theta^2) (2\bar{V}_r - \bar{V}_\theta \cot \theta)}{\left[\frac{\gamma-1}{2} (1 - \bar{V}_r^2 - \bar{V}_\theta^2) \right] - \bar{V}_\theta^2} \quad (2)$$

$$\bar{V} = \frac{V}{V_{\max}} = \frac{V}{\sqrt{2C_p T_{o_\infty}}} \quad V_\theta = \frac{dV_r}{d\theta} \quad (3,4)$$

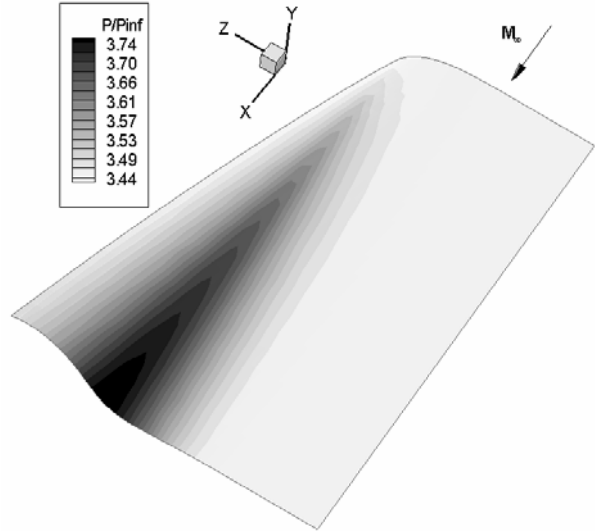


Figure 2: Pressure distribution on half of the lower surface of an uncorrected osculating cone

This ordinary differential equation is readily integrated, in the present work with a fourth-order Runge-Kutta method. In the basic osculating cones solution, the flowfield is defined from a prescribed shockwave and intersecting leading edge; in the present work, powerlaw functions are used for simplicity. Local tangent, or “osculating” cones are traced along the prescribed shockwave shape at each discrete point. The radius of the osculating cone is just the local radius of curvature of a virtual generating surface. The intersection of the prescribed leading edge curve and the local osculating shock has to be determined. The longitudinal position of the leading edge is determined by projecting the previous leading edge point in the streamwise direction: the vehicle leading edge occurs at the intersection of the shockwave surface generated by the local osculating cone and the proscribed leading edge curve. The upper surface of the vehicle is then obtained by projecting each leading edge point downstream to the base plane. The entire shockwave is determined by marching upstream along each local osculating cone surface.

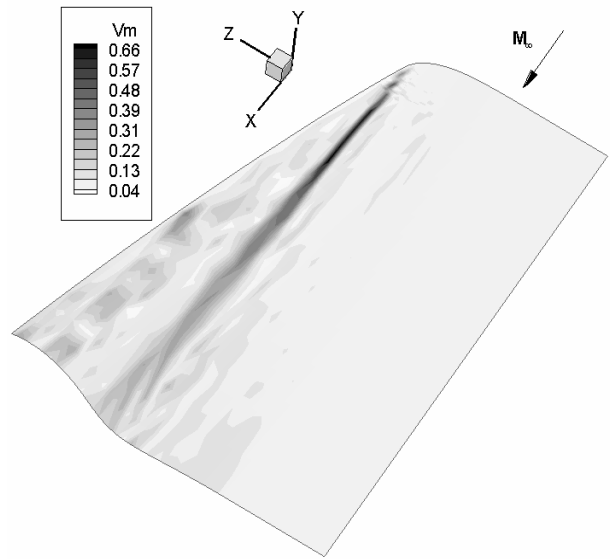


Figure 3: Velocity correction amplitude on half of the lower surface of an osculating cone design.

B. Osculating-Cone Solutions

In recent efforts, a simple predictor-corrector algorithm has been applied using Euler’s flow equation to modify velocity, imposing a crosswise velocity component away from the gradient: $dV = -dp/\rho V$. Some recent results are shown in Fig. 3, which presents the magnitude of corrected velocity on an osculating cone waverider lower surface. In all cases examined thus far, the magnitude of the correction has been small, and so may actually be neglected with negligible impact on overall waverider performance. These solutions are currently being developed with transonic drag considerations, using the classic area rule to minimize transonic drag while seeking good hypersonic performance.

C. Lifting Versus Vertical Launch

The corrected waverider designs and similar efforts are all being developed with an eye towards application to future generation space vehicles. There is a fundamental question as to whether lifting bodies will ultimately provide improved access to space, as compared to more traditional approaches. To this end, work at the SVT Institute over the past year has addressed the basic question of aerodynamic launch versus vertical launch, with an eye to overall performance benefits. This includes the evaluation of overall aerodynamic performance, weight and volumetrics, and tradeoffs between wing and landing gear combinations and engine performance.

As indicated above, the performance of vertical launchers is constrained by gravity losses and the engine weight requirements for associated with having thrust greater than weight. Horizontal launchers can have lighter-weight propulsion systems because lift is countering weight, and, if airbreathing, will have much higher specific impulse than their rocket counterparts. Horizontal vehicles will have wings and landing gear that may add considerable weight to the overall craft.

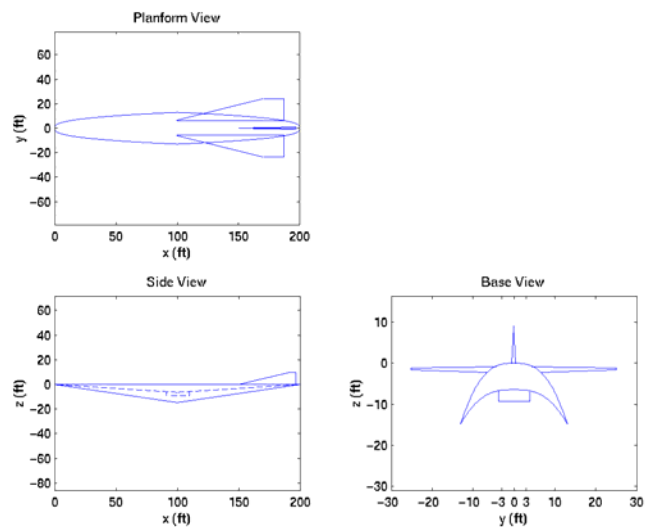


Figure 4 Parametric geometry model for first stage of a horizontal TSTO launch vehicle, with wing and body sizes and weights.

There is an extensive historical database upon which to draw for modeling conventional rocket weights. Similarly, there are substantial data available for predicting conventional aircraft weights across the spectrum of aircraft sizes and mission models. However, there are of course no historical antecedents for the modeling of a horizontal launcher, and only a few analogous aircraft types from which to draw comparisons.

A horizontal launcher will likely have gross takeoff weights in the million pound range, limited by runway capabilities. This means that a horizontal launcher will likely be larger than a 747-400 (maximum takeoff weight =910,000 lb.) or a C-5 Galaxy (840,000 lbs.), and comparable to the Russian Antonov-225 (max. weight=1,300,000 lbs.). The vehicle will likely have blended wing-body configuration for effective high-speed performance, with very high takeoff speeds. Thus, predicting required wing sizes and weights must rely on a combination of extrapolated data and analytical modeling.

Efforts have focused on building a parametric model for a horizontal two-stage-to-orbit (TSTO) launcher with an airbreathing first stage and conventional second stage. A database of design and component weights for existing vertical launch vehicles and aircraft similar in size or performance to a typical horizontal launch vehicle is being developed to look at the weight penalties incurred by each system. Isolating the weight penalties associated with a blended lifting body, as opposed to a simple rocket scheme, is especially challenging.

Current focus has been on developing the first stage airbreather of the horizontal TSTO model seen in Fig. 4 below. The fuselage forebody and aftbody are based on power-law derived planar shock waverider geometries, optimized for the best combination of lift-to-drag and volumetric efficiency at a design point of Mach 10, 100,000 feet altitude, zero degree angle of attack, maximum length of 200 feet, maximum width of 120 feet. Aerodynamic modeling is used to size the wings for takeoff; a tail is sized for lateral stability and control.

Ongoing work is continuing to develop a weights database for various vertical launch vehicles and aircraft as well as the calculation of representative metrics to be used in direct comparison of different launch systems. The parametric horizontal TSTO model will be continually upgraded to eventually include the second stage and also things like center of pressure and moment calculations, an airbreathing engine model, trajectory and staging considerations, fuel selection, landing gear placement, etc. Another important issue is landing gear weight, especially if sized properly to account for maximum takeoff speeds. This requires a database that not only accounts for gear weight as a function of maximum takeoff weight, but which also correlates gear weight to low-speed aerodynamic performance.

III. Fundamental Studies

A. Sharp Leading Edges

The basic premise of the high-lift configurations described above depends on the effective use of slender body aerodynamics with sharp leading edges. The understanding of the physics of flow on high-speed leading edges is a primary topic of research in the Space Vehicle Technology Institute.

Prior theoretical and analytical studies have focused attention on different flight regimes. For example, O'Brien and Lewis²⁰ considered very low altitude,

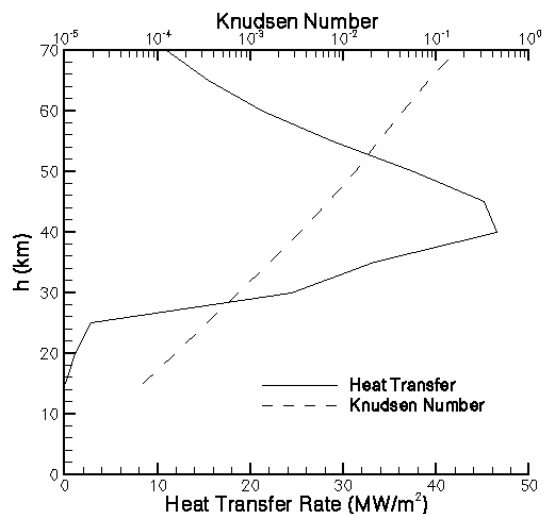


Figure 5. Profiles of stagnation point heating and Knudsen number on a representative, air-breathing launch trajectory

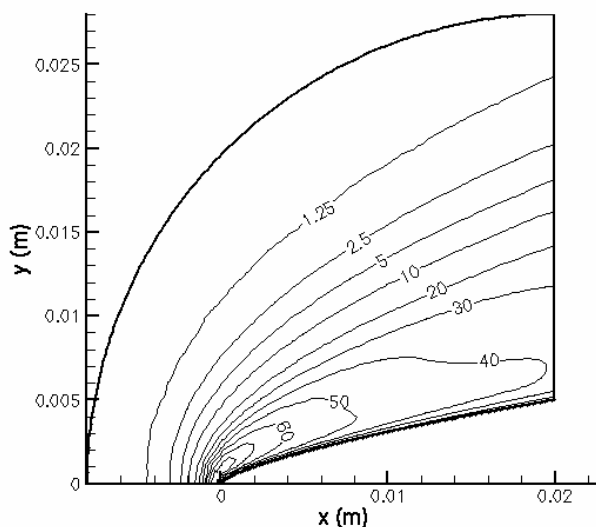


Figure 6. Contours of temperature ratio (T/T_∞) for flow around the $n=0.7$ power-law shape at $U_\infty=7.5$ km/s.

inviscid conditions by solving the Euler equations, while Santos and Lewis^{21,22} applied the direct simulation Monte Carlo method (DSMC)²³ to study high altitude, rarefied conditions. Recent work is pursuing the next step: a more comprehensive computational analysis, using various numerical methods, of the aerodynamic performance of sharp leading edges across the full range of conditions experienced in a representative flight trajectory. The assessment should involve comparisons of heat transfer, drag force, and shock standoff distance, for a variety of on- and off-design points.

To first order, the trajectory of an air-breathing hypersonic reusable launch vehicle is designed to provide pressures inside the propulsion system to be a sizeable fraction of atmospheric pressure in order to achieve efficient combustion. Figure 5 provides profiles of stagnation point heat flux and Knudsen number for the representative trajectory of Bertin²⁴. The heat flux in MW/m² is determined using the following correlation of Detra et al.²⁵:

$$\dot{q} = \frac{110.3}{\sqrt{R_N}} \sqrt{\rho} \left(\frac{U}{U_{CO}} \right)^{3.15} \quad (1)$$

where R_N is the nose radius, taken to be 5 mm representative of the sharp leading edges of interest in this study, ρ_{SL} is sea-level mass density, and U_{CO} is the orbital velocity (taken to be 7.95 km/s). The Knudsen number is computed using a constant, hard-sphere collision cross section, and a characteristic length of 5 mm. Note that, as the vehicle descends through the atmosphere, the Knudsen number decreases from the rarefied flow regime (10^{-1}) through the transition regime into the continuum flow regime (10^{-4}). While the region of maximum heat flux (around 40 km) has a Knudsen number in the near-continuum regime (about 5×10^{-3}), the local radius of curvature on a sharp leading edge may be smaller than the gross dimension of 5 mm thus increasing the local Knudsen number. Hence, the overall assessment of sharp leading edges for such vehicles requires both continuum and rarefied flow analyses. The continuum regions can be analyzed using the Navier-Stokes equations and the rarefied regions must be computed using a kinetic approach such as the DSMC technique. Note that the classic methods for predicting flow properties at the leading edges of slender hypersonic bodies, including thin shock layer theory and blastwave analogies, fail for very sharp leading edges, where it is most important to predict heating rates. As such, numerical solutions are being pursued.

Work in the SVT Institute has used DSMC to compute rarefied hypersonic flows around representative sharp leading edges. Among the results have been a quantitative comparison of the effects of sharpening a leading edge. Comparisons between simply cylinders and powerlaw leading edge shapes, defined by the function $y = Ax^n$, have been made. Representative temperature ratios around a powerlaw leading edge with $n=0.7$ are shown in Fig. 6.

Work thus far has revealed significant

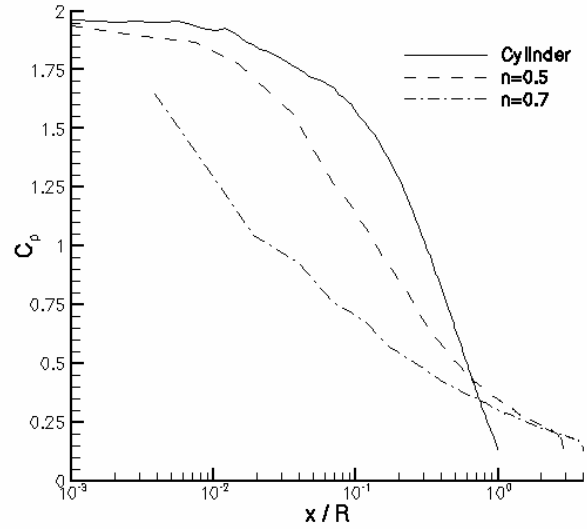


Figure 7. Surface profiles of pressure coefficient around leading edge shapes at $U_\infty = 7.5$ km/s.

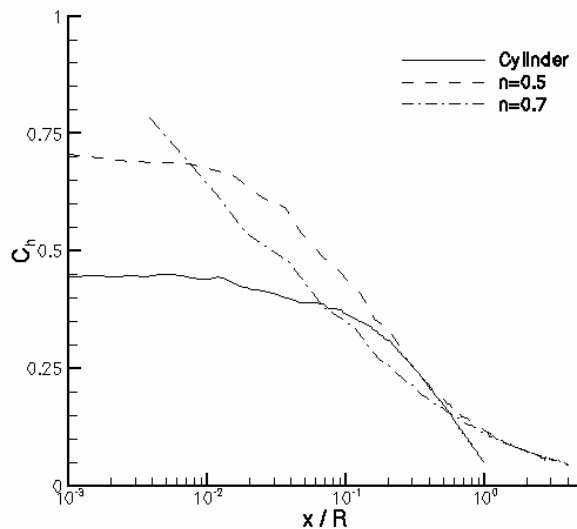


Figure 8. Surface profiles of heat transfer coefficient around various leading edge shapes at $U_\infty = 7.5$ km/s.

reductions in the stagnation point density as the leading edge is sharpened from a cylinder to a powerlaw of $n=0.5$, then $n=0.7$, though the shock is barely detached for the $n=0.7$ shape. Minimization of the shock standoff distance is desirable to avoid flow spillage around the upper surface of the leading edge that would decrease lift on a wing and decrease engine inlet flow rate on a cowl lip, both of which reduce the vehicle efficiency. Surface properties including pressure, skin friction, and heat transfer, have been calculated.

Note that it is difficult to obtain information at very small x coordinate for the $n=0.7$ power-law shape due to its very sharp profile. It should be noted that the mesh resolution employed in this case at the tip has involved cells that are much smaller than the local mean free path. The profiles of the coefficient of pressure presented in Fig. 7 indicate similarities between the cylinder and $n=0.5$ cases, and each of these is close to the Newtonian model. The $n=0.7$ case is very different as the pressure does not reach its stagnation value at the tip. The sharper shape of the $n=0.7$ power-law leads to increased friction and heat transfer at the tip. Figure 8 presents heat transfer coefficient profiles along the surfaces. This would have great significance for a sharp leading-edged high-speed vehicle.

A summary plot of the data for shock standoff distance normalized by the body radius, (Δ/R) , and maximum heat transfer coefficient are shown in Fig. 9. These data clearly illustrate the advantages and disadvantages of sharper leading edge shapes.²⁶ With the $n=0.7$ power-law shape, the shock standoff distance is reduced almost to zero, but this is accompanied by a factor of two increase in maximum heat transfer coefficient.

B. Plasma Effects

Another fundamental topic receiving attention in the SVT Institute with important implications for next generation space vehicles is the plasma environment in the shock layer, especially during reentry. The focus here is on understanding ionization effects in the shock layer to enable communication through all phases of flight. It will be of particular interest to avoid communications blackouts during reentry for safety and guidance. For instance, with continuous telemetry through reentry GPS could be used for a maneuvering landing. Telemetry through a plasma is also important for commanded destruction during flight test, for instance for a horizontal launcher.²⁷

The approach of this work has been to model the flow once again using a direct numerical method that includes ionization and electromagnetic effects. It is of interest to first map out the ionization fractions in the shock layer in a sharp leading edge region. The idea is that the high heating rates associated with such geometries will likely concentrate most of the ionization near the front of the vehicle, so transmission may be possible near the base.

In order to penetrate the plasma layer, it is necessary to have a transmission frequency that is greater than the plasma frequency. Preliminary calculations at Mach 14, 60 km suggest plasma frequencies of about 120 GHz at the leading edge, but dropping quickly into the tens of GHz further downstream. It has also been found that collision frequencies are generally orders of magnitude higher (temperature) or lower (electron-electron) than typical

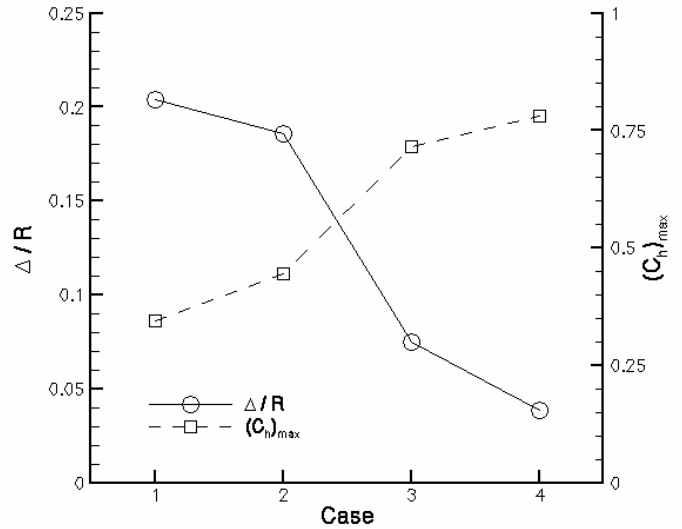


Figure 9. Summary of shock standoff and maximum heat transfer coefficient data for all cases considered.

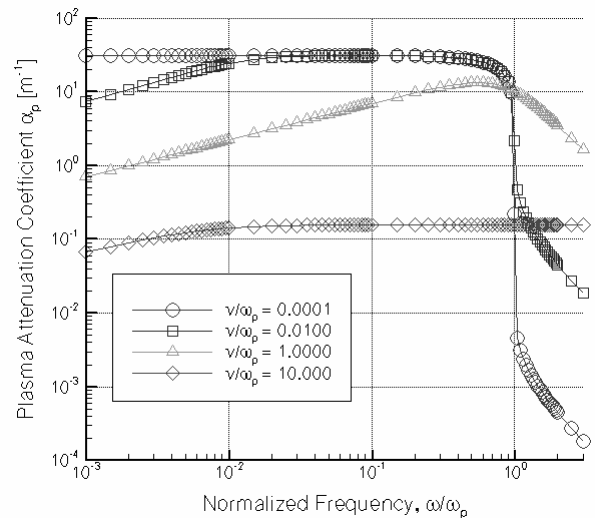


Figure 10. Attenuation coefficient through a Mach 14 shock layer at 60 km, as a function of radio frequency. From Ref. 27.

transmission values, and should have little effect on attenuation and telemetry. This work is also benefiting from plasma activities for propulsion applications in the SVT Institute.

C. Inward Turning Inlets.

In the area of applied aerodynamics, there has been a focus of efforts in the SVT Institute on three-dimensional inlets – departing from the “classic” spatulate forms chosen for vehicles such as the National Aerospace Plane.²⁸ Whereas these spatulate shapes are designed to offer primarily 2-D flow into an airbreathing engine with reduced drag, three-dimensional shapes may offer significant packaging and aerothermal advantages.²⁹

Building on inverse-design approaches, this work has been aimed at developing 3-D forebodies that provide desired flow properties to an engine inlet plane. As with the waverider, the idea has been to exploit the mathematically-hyperbolic nature of supersonic flow, defining desired downstream conditions and then marching upstream to the shockwave that will provide them. The new aspect of this work is that the inward turning design is a compression flowfield with converging streamlines. This does not lend itself to using streamsurfaces that are carved from wedge-derived or even conical shock solutions. This work builds on the research of Kothari and Tarpley, et. al.

The approach under pursuit has been to apply the classic method of characteristics to march upstream of a defined inlet plane. In essence, the initial flowfield is solved like a nozzle, then the direction of flow is reversed. In inviscid flows, the thermodynamic properties and velocity magnitudes will be the same. At the shockwave, the Rankine-Hugoniot equations are solved backwards – a solution is sought which provides a desired pressure drop (as observed moving upstream) subject to a given flow direction. The shock must be chosen so that the freestream is completely uniform in pressure and velocity, so that when the flow is reversed it correctly represents a forebody flying into undisturbed free-stream.

A preliminary example of this is shown in Fig. 10, from the work of Barkmeyer. An upper surface has been added to the compression surface by aligning to freestream streamlines and projecting downstream. This inlet represents a new class of inversely-derived waverider, though there are clearly many questions that must be answered before it would be accepted for practical use.

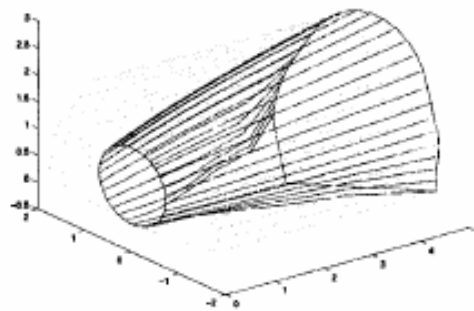


Figure 10. Inward turning forebody for 3-D compression into a uniform inlet plane.

IV. Conclusions

High-speed aerodynamics research represents a significant effort in the Space Vehicles Technology Institute. Topics cover a wide range of problems, from highly applied inlet studies and optimal airframes, to very fundamental studies of high-speed leading edge flows and plasma effects. Research projects outlined in this work represent just a small fraction of the total activities in the SVTI, many of which relate in some manner to aerodynamics and engine integration, even if that is not their explicit objective. This includes engine cycle analysis, flowpath-related studies, high-temperature materials, and aeroelasticity. Additional work on plasmas for flow control and computational modeling are also directly relevant to launch vehicle aerodynamics and integration. All of these projects have as their goal the development of understanding with direct relevance to future launch vehicles, with guidance from NASA and DoD sponsors.

Since the initiation of the University Institute program, NASA interests have been redirected from the NGLT program towards the President’s Moon-Mars Exploration Initiative. In response to this, activities throughout the consortium will be refocused in the coming year to address topics of relevance to Moon-Mars exploration. This will include a de-emphasis of airbreathing options (though not a total termination, in response to DoD interests) and renewed interest in more traditional rockets and space vehicles that operate beyond the confines of earth orbit.

Acknowledgments

This work has been sponsored by the NASA-University Institute program, with joint support from the Department of Defense, Grant NCC-3989. Claudia Meyer of the NASA Glenn Research Center is program manager, and appreciation is expressed for her efforts, as well as to of Mark Klem and Harry Cikanek, also of NASA Glenn.

Appreciation is also expressed to Dr. John Schmisser and Dr. Walter Jones of the Air Force Office of Scientific Research, and Dr. Ken Harwell, Special Assistant to the Director, Defense Research and Engineering.

References

- ¹ Lewis, M. J. "Significance of Fuel Selection for Hypersonic Vehicle Range," *JPP*, Vol. 17, No. 6, Nov.-Dec. 2001 pp. 1214-1221.
- ² O'Neill, M.K., and Lewis, M.J., "Optimized Scramjet Integration on a Waverider," *JoA*, Vol. 29, No. 6, Nov.-Dec., 1992, pp. 1114-1121.
- ³ Lewis, M. J. "Lift Requirements for Airbreathing Flight to Orbit" AIAA-2002-5113 11th AIAA/AAAF International Conference on Space Planes and Hypersonic Systems and Technologies Orleans, France Sept. 29-Oct. 4, 2002.
- ⁴ Huebner, L.D., Rock, K.E., Witte, D. W., Ruf, E.G., Andrews, E.A., "Hyper-X Engine Testing in the NASA Langley 8-foot High Temperature Tunnel," AIAA Paper 2000-3605, presented at the 36th AIAA/ASME/SAE/ASEE Joint Propulsion Conference and Exhibit, Huntsville, AL, July 16-19, 2000.
- ⁵ Cockrell, C., Merski, R., Witte, D., and Mulqueen, J., "Aerosciences, Aero-Propulsion and Flight Mechanics Technology Development for NASA's Next Generation Launch Technology Program," AIAA Paper 2003-6948 presented at the 12th AIAA International Space Planes and Hypersonic Systems and Technologies, Norfolk, VA Dec. 15-19, 2003.
- ⁶ Moses, P., "NASA Hypersonic Propulsion Flight Demonstrators - Overview, Status, and Future Plans," IAC-03-V.6.01 presented at the 54th International Astronautical Congress, Bremen, Germany, Sept. 29-Oct. 3 2003.
- ⁷ Witte, D., Huebner, L., Trexler, K., Cabell, K., and Andrews, E., "Propulsion-Airframe Integration Test Techniques for Hypersonic Airbreathing Configurations at Langley Research Center," AIAA Paper 2003-4406, presented at the 39th AIAA/ASME/SAE/ASEE Joint Propulsion Conference and Exhibit, Huntsville, AL July 2003.
- ⁸ Bordelon, W, Frost, A., and Reed, D., "Stage Separation Wind Tunnel Tests of a Generic TSTO Launch Vehicle," AIAA Paper 2003-4227, presented at 21st AIAA Applied Aerodynamics Conference.
- ⁹ Kimmel, R., "Aspects of Hypersonic Boundary Layer Transition Control," AIAA 2003-772, presented at the 41st Aerospace Sciences Meeting and Exhibit, Reno NV, Jan. 2003.
- ¹⁰ Bertelrud, A., de la Tova, G., Hamory, P.J., Young, R., Noffz, G.K., Dodson, M., Graves, S.S., Diamond, J. K., Bartlett, J. E., Noack, R., and Knoblock, D., *Pegasus® Wing-Glove Experiment to Document Hypersonic Crossflow Transition—Measurement System and Selected Flight Results*, NASA-TM-2000-209016, CA, January 2000.
- ¹¹ Jiang, L., Choudhari, M., Chang, C., and Liu, C., "Direct Numerical Simulations of Crossflow Disturbances in Supersonic Boundary Layers," AIAA Paper 2004-589, presented at the 42nd AIAA Aerospace Sciences Meeting and Exhibit, Reno, NV Jan. 2004.
- ¹² Berry, S., Nowak, R., and Horvath, T. "Boundary Layer Control for Hypersonic Airbreathing Vehicles," AIAA 2004-2246, presented at the 34th AIAA Fluid Dynamics Conference and Exhibit, Portland, OR, July 2004.
- ¹³ Smart, M., "Design of Three-Dimensional Hypersonic Inlets with Rectangular to Elliptical Shape Transition, AIAA 98-0960, presented at the AIAA Aerospace Sciences Meeting, Reno, Nev. Jan. 1998.
- ¹⁴ Sabeen, J., and Lewis, M.J. "Computational Optimization of a Hypersonic Rectangular-to-Circular Inlet," *JPP*, Vol. 17, No. 3, May-June 2001 pp. 571-578.
- ¹⁵ Nonweiler, T.R.F. "Delta Wing Shapes Amenable to Exact Shockwave Theory," *J.Roy.Aero.Soc.*, Vol. 63, 1959, pp. 521-528.
- ¹⁶ Starkey, R, and Lewis, M.J., "A Simple Analytical Model for Parametric Studies of Hypersonic Waveriders," *JSR*, Vol. 36, No. 4, July-August 1999, pp. 516-523.
- ¹⁷ Takashima, N., and Lewis, M.J., "A Cone-Wedge Waverider Configuration for Engine-Airframe Integration," *JoA*, Vol. 32, No. 5, pp. 1142-1144, September-October 1995.
- ¹⁸ Takashima, N., and Lewis, M. J., "Optimization of Waverider-Based Cruise Vehicles with Off-Design Considerations," *J.ofA.*, Vol. 36, No. 1, Jan-Feb 1999, pp. 235-245.
- ¹⁹ Taylor, G.I. and Maccoll, J.W., "The Air Pressure on a Cone Moving at High Speed", *Proc.Roy.Soc.*:278-311, 1933.
- ²⁰ O'Brien, T.F. and Lewis, M.J., "Power-Law Shapes for Leading-Edge Blunting With Minimal Shock Standoff," *Journal of Spacecraft and Rockets*, Vol. 36, 1999, pp. 653-658.
- ²¹ Santos, W.F.N. and Lewis, M.J., "Power-Law Shaped Leading Edges in Rarefied Hypersonic Flow," *Journal of Spacecraft and Rockets*, Vol. 39, 2002, pp. 917-925.
- ²² Santos, W.F.N. and Lewis, M.J., "Aerodynamic Heating Performance of Power-Law Shaped Leading Edges in Rarefied Hypersonic Flow," AIAA 2003-3894, AIAA Applied Aerodynamics Meeting, June 2003.
- ²³ Bird, G.A., *Molecular Gas Dynamics and the Direct Simulation of Gas Flows*, Oxford Science, New York, 1994.
- ²⁴ Bertin, J.J., *Hypersonic Aerothermodynamics*, AIAA Press, 1994, p. 2.
- ²⁵ Detra, R.W., Kemp, N.H., and Riddell, F.R., "Addendum to Heat Transfer to Satellite Vehicles Reentering the Atmosphere," *Jet Propulsion*, Vol. 27, 1957, pp. 1256-1257.
- ²⁶ Boyd, I.D. and Padilla, J., "Simulation of Sharp Leading Edge Aerothermodynamics," AIAA 2003-7062, December 2003.
- ²⁷ Hoult, D., Starkey, R. P., and Lewis, M. J., "DSMC of Power-Law Leading Edge Ionization for Hypersonic Telemetry Applications" AIAA 2003-6964, 12th International Space Planes and Hypersonic Systems and Technologies Conference, Norfolk, VA, Dec 15-19, 2003.
- ²⁸ Lewis, M.J., "Designing Hypersonic Inlets for Bow Shock Location Control," *JPP*, Vol. 9, No. 2, pp. 313-321, March-April 1993.

²⁹Kothari, A.P., Tarpley,C., Raghavan,V., and Livingston, J. W., “Comparison of Inward and 2D SSTO/TSTO and HTHL/VTHL Vehicles for Access-to-Space”, 2002 JANNAF, Lake Buena Vista, FL, Nov 2002.